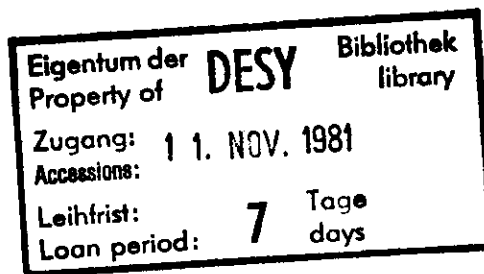


Internal Report  
DESY D3/38  
September 1981

ABSORBED DOSE AND ENERGY DEPOSITION CALCULATION DUE TO  
SYNCHROTRON RADIATION FROM PETRA, HERA AND LEP

by

Chiri Yamaguchi



**DESY behält sich alle Rechte für den Fall der Schutzrechtserteilung und für die wirtschaftliche Verwertung der in diesem Bericht enthaltenen Informationen vor.**

**DESY reserves all rights for commercial use of information included in this report, especially in case of filing application for or grant of patents.**

**“Die Verantwortung für den Inhalt dieses  
Internen Berichtes liegt ausschließlich beim Verfasser“**

Internal Report  
 DESY D3/38  
 September 1981

Absorbed Dose and Energy Deposition Calculation Due to  
 Synchrotron Radiation from PETRA, HERA and LEP

by  
 Chiri Yamaguchi

ABSTRACT

The Monte Carlo code EGSJ has been used to calculate the absorbed dose due to synchrotron radiation. The dose to RPL glass dosimeters located in the air gaps of a dipole magnet and the radial dose distribution in the PETRA tunnel have been obtained. The results are compared with the values measured by Dinter and Tesch. The photon energy spectrum in various regions of the magnet gap is given. Similar calculations have been done for HERA and LEP. The absorbed dose and energy deposition fractions in various components of the dipole magnet are given as a function of the thickness of the lead shield. The radial dose distribution in the LEP tunnel are also presented. Some results for HERA are compared with the calculated values reported by Kötzt.

(To be submitted partly to Nucl. Instr. and Methods)

1. INTRODUCTION

When a charged particle moves on a circular orbit with a highly relativistic velocity, it emits electromagnetic radiation generally known as synchrotron radiation. It has a continuous spectrum which, e.g. in the case of PETRA energy regions, ranges from infrared to the hard x-ray region of a few hundred keV. It is highly directional and is emitted along a tangent to the circulating particle orbit in a narrow cone of the angle  $m_0 c^2/E$  in the laboratory system, where  $m_0$  is the rest mass and  $E$  is the energy of the particle.

The photon spectral density is given by Schwinger<sup>1)</sup> as follows:

$$\frac{d^2N}{dE \cdot dt} = \frac{5.320 \times 10^{11}}{[E(\text{GeV})]^2} G(x) \quad (\text{photons MeV}^{-1} \text{s}^{-1}) \quad (1)$$

$$\frac{d^2N}{dE \cdot d\ell} = \frac{17.75}{[E(\text{GeV})]^2} G(x) \quad (\text{photons MeV}^{-1} \text{m}^{-1}) \quad (2)$$

where  $G(x)$  is the integral of a modified Bessel function  $K_{5/3}$ , and it is expressed as:

$$G(x) = \int_x^\infty K_{5/3}(t) dt, \quad x = \frac{E}{E_c}$$

The energy  $E_c$  in the above equation is called critical energy and it is defined as the energy below which half of the total power is radiated and half above. In equation it is expressed as:

$$E_c = 2.218 \frac{[E(\text{GeV})]^3}{R(\text{m})} \quad (3)$$

The radiation power loss  $\Delta E$  per revolution of an electron in a circular orbit of radius  $R$  is expressed as follows:

$$\Delta E(\text{keV}) = \frac{88.46 [E(\text{GeV})]^4}{R(\text{m})} \quad (4)$$

The synchrotron radiation strikes the water-cooled outer wall of the vacuum chamber at a small grazing angle of 24 mrad in PETRA and 7 mrad in LEP. A great amount of the synchrotron radiation is absorbed at this position resulting an ionization of cooling water. The scattered gamma radiation brings the formation of ozone in the air of the tunnel and radiation damage to various accelerator equipments. Adding a few mm thick lead shielding around the vacuum chamber reduces the absorbed dose in the tunnel to a great extent.

Some measurements of absorbed dose due to the synchrotron radiation in the PETRA tunnel have recently been reported by Dinter and Tesch<sup>2)</sup>. The present work deals with the absorbed dose calculation for the measurements using the electromagnetic shower EGS program developed by Ford and Nelson<sup>3)</sup>. It also provides some other absorbed dose calculations from the synchrotron radiation for the forthcoming projects HERA (Hamburg) and LEP (Geneva).

## 2. DOSE CALCULATION

### 2.1 Concept of dose calculation

The EGS Code system (version 3), referred as EGS3, is a package of computer programs that simulates the development of electromagnetic cascade showers in various media using the Monte Carlo method. It outputs the fraction of energy deposited in various regions of interest. The user is required to prepare his own MAIN user code and a geometry subroutine HOFAR and an output subroutine AUSGAB.

A new MAIN user code has been prepared<sup>4)</sup> to obtain the photon spectrum and to calculate the absorbed dose in the air region from it. When the radiation equilibrium between primary photons and secondary electrons is established, the absorbed dose  $D$  (rad) of a material exposed to gamma radiation is given by<sup>5)</sup>

$$D = 1.60 \cdot 10^{-8} \sum_i \phi_i E_i \left( \frac{\mu_{en}}{\rho} \right)_i t, \quad (5)$$

where,

- $\phi_i$  = the flux density in  $\text{cm}^{-2}\text{s}^{-1}$  for the  $i$ -th photon in the region of interest (ROI),
- $E_i$  = the energy of the  $i$ -th photon in MeV,
- $(\mu_{en}/\rho)_i$  = mass energy absorption coefficient in  $\text{cm}^2 \text{g}^{-1}$  for the  $i$ -th photon in the medium, and it is a function of photon energy,
- $t$  = exposed time in s.

The mass energy absorption coefficient  $\mu_{en}/\rho$  is expressed as follows:

$$\frac{\mu_{en}}{\rho} = \frac{1}{\rho} \left[ \tau (1-f) + \sigma \frac{\bar{E}}{h\nu} + \kappa \left( 1 - \frac{2mc^2}{h\nu} \right) \right] (1-G), \quad (6)$$

where

- $\tau$  = photoelectric cross section,
- $\sigma$  = total Compton cross section,
- $\kappa$  = pair production cross section,
- $f$  = fluorescent x-ray fraction,
- $G$  = fraction of energy lost by secondary electrons, in bremsstrahlung processes

Thus, in the present calculation whenever the term absorbed dose in the "air" region appears, e.g. the region at a certain distance from the magnet, it represents the absorbed dose in the RPL (radiophotoluminescent) glass dosimeter which shall be located in the region. This is confirmed by the fact that we are generally interested in the absorbed dose in various accelerator equipments and most of which can be well represented by aluminum whose mass energy absorption coefficient is very much similar to that of the glass dosimeter<sup>6)</sup>.

In eq. 5 the term  $\phi_i E_i$  gives energy flux density for the  $i$ -th photon with its energy  $E_i$ , and the product  $\phi_i E_i (\frac{\mu_{en}}{\rho})_i t$  is equal to Kerma (kinetic energy released to matter), when fraction of energy lost by secondary electrons in bremsstrahlung processes is negligible (i.e.  $G = 0$ ). When the radiation equilibrium is not established, the calculated Kerma values overestimate the actual absorbed dose to some extent. In the main user code the average value of mass energy absorption coefficient for RPL glass is used for each of the energy

bins which the user has to specify. The mass energy absorption coefficient for the glass dosimeter has been calculated from the table of ref. 7 based on its elemental composition.

When the photons are coming into a region homogeneously from every direction, the photon flux density can be expressed as the number of photons per unit time that pass through a sphere which has a unit cross-sectional area. In the present calculation, however, the photon flux density  $\phi_i$  in eq. 1 for the region of interest (ROI) which was filled with air was calculated assuming that the photons were coming into the region from one side (x-y plan in Fig. 1). The x, y and z dimensions of each ROI in the calculation for PETRA were  $1.6 \times 1.6 \times 2.0 \text{ cm}^3$ . (The dimension in x-direction can actually be any length because the absolute number of photons per any magnet length that hit the vacuum chamber wall can be obtained easily.) This assumption overestimates the photon flux density by a factor of 1.5 when the photons are coming into the ROI homogeneously. (The factor is reduced to 1.3 when the region is a cube.)

The output values of the program which give the fraction of energy deposited in each region and the Kerma for the specified regions are normalized to one electron (or positron) and one m of a magnet length. Thus the final figures that give the absorbed dose to the ROI are obtained by multiplying the Kerma by the synchrotron radiation energy loss per m and the total number of the electrons and positrons.

Some useful parameters concerned with the synchrotron radiation from PETRA, HERA and LEP are listed in Table 1. The necessary data for the calculations have been taken from ref. 8 for HERA and from the Pink Book<sup>9)</sup> and a recent note<sup>10)</sup> for LEP.

## 2.2 Geometry in calculation

The measurement positions of the synchrotron radiation in the PETRA dipole magnet gap are given in ref. 2. The corresponding geometry used in the present calculation is shown in Fig. 1. The

figure depicts a cross section of the PETRA dipole magnet on y-z plane. The magnet is assumed to be infinitely long in x-direction, and the simulation of electromagnetic shower transportation is carried out three dimensionally. Each region is filled with the corresponding materials such as iron, aluminum, lead, air or vacuum. The synchrotron radiation hits the inside wall of the vacuum chamber with an incident angle of 24.4 mrad toward x-direction. The figure is not drawn in linear scale. The shielding effect of the distributed ion pump in the vacuum chamber has been taken into account by increasing the effective thickness of the vacuum chamber wall.

The geometries used in the calculation for HERA and LEP are shown in Figs. 2 and 3, respectively. The radial dose distribution in the tunnel was calculated by using the slightly modified geometries given in ref. 4.

## 2.3 Computer and computing time

Two IBM/370-168 and one IBM/3033 central processing machines are installed at DESY. They are operated by NEWLIB/TSO time sharing system. Each job was run for 16 min IBM/370-168 equivalent CPU time. In order to check a stochastic variation in the results the job with equal geometrical parameters was repeated at least three times by changing the random number generation seed. In the case of PETRA the calculation was repeated 25 times, or 400 min CPU time was provided.

## 3. RESULTS OF CALCULATION

### 3.1 PETRA

#### 3.1.1 Absorbed dose in the dipole magnet air gap

The results of the calculation for the measurements by Dinter

and Tesch are compared in Table 2. The figures are expressed in rad and are normalized to an integrated current of 100 mA h. The corresponding figures agree with each other within a factor of two, which is very good in the complicated Monte Carlo calculation. Since the energy flux density was calculated assuming that the photons were emerging the brick geometry through one side, as stated in section 2.1, the calculated values were overestimated by a factor of 1.5 when the photons were coming into the regions of interest homogeneously from every direction. The photon distribution around ROI = C and A showed more or less this tendency, which explains partly the discrepancy between the calculation and measurement values for these regions. The standard deviations of the calculated results which were obtained by 25 runs of the program with different random generation seeds are also given in the table. Since the errors of the complicated Monte Carlo calculation cannot simply be measured by the standard deviation, they only give a criterion of the error estimation.

Table 3 shows the deposited energy fraction of the synchrotron radiation power from PETRA in the various accelerator components. A great amount of the synchrotron radiation power is absorbed in the vacuum chamber, i.e. 70% at 17 GeV operation and 54% at 21 GeV. Further, the energy deposition in the vacuum chamber is performed at the wall and "nose" of the chamber where the synchrotron radiation directly hit the chamber. This amounts 88% in 17 GeV and 92% at 21 GeV. This can be seen from Fig. 5 in which detailed deposited energy fractions in the vacuum chamber and the lead shields in its both sides are shown.

### 3.1.2 Photon energy fraction spectra

Fig. 4 gives the energy fraction spectra for the regions in the dipole magnet air gap where the RPL glass rods were located.

Each step of the histogram shows a fraction of energy per energy bin to the total energy of the synchrotron radiation. The sum of the height for the individual energy bins of the histogram for the input spectrum is normalized to unity. The spectrum for ROI = B is one just outside the vacuum chamber wall which the synchrotron radiation hits. Although the photons impinge almost parallel to the wall and its "effective" thickness seems very large, the higher energy components are still not absorbed. The photons with lower energies than 30 keV are all absorbed before they come out of the vacuum chamber. The main contribution to the energy fraction is from the photons with energies between 60 and 150 keV. The spectrum for ROI = A shows that after the 3 mm lead shield, the photons are greatly absorbed. Even photons with higher energies are absorbed by a factor of 10 to 100. The contribution from the photons with energies between 60 and 200 keV is reduced by a factor of 1000. The photons whose energies are lower than 50 keV are not observed.

The spectrum for ROI = C which is the region inside the beam orbit has a similar shape to that for ROI = B, the outside region, but the former is degraded by a factor of 100 (in higher energy region) to a few hundreds (in lower energy region). The highest contribution to the energy fraction is from the 100 to 150 keV energy bin. This spectrum, after passing through the 3 mm lead shield, changes its shape to: ROI = D. The latter spectrum consists of photons whose energies are larger than 60 keV, but, the energies of the most photons are between 150 and 300 keV. Thus, the photons outside the lead shield are hard x-rays.

### 3.1.3 Radial absorbed dose distribution

The special absorbed dose distribution at beam height in the radial direction in the PETRA tunnel was also calculated. The geometry used in the calculation is shown elsewhere<sup>4)</sup>. The individual air regions for which the dose was calculated had y x z dimensions of 10 x 10 cm<sup>2</sup>. Fig. 6 shows the results both with and without adding a 3 mm thick lead shield on both sides of the vacuum chamber in the

PETRA dipole magnet. The vertical lines indicate the variation of the values in several computer runs, and the points are their arithmetic mean values. The distance,  $r$ , is measured from the surface of the vacuum chamber.

In both cases the calculated points are well fitted by a function expressed as  $(1/r)^{0.8}$ . The above results were compared with the measured values of ref. 2. Since the shielding with lead plates of some accelerator parts, i.e. vacuum flanges, bellows etc., is not complete, we cannot take the values calculated for the completely shielded case. The contribution of the radiation escaping through the incompletely shielded parts must be taken into account. The more complete the shielding, the more prominent its contribution. The comparison between measurement and calculation is shown in Fig. 7. The solid line was drawn by the eye. The calculated data corresponds to the situation that 3% of the total accelerator ducts is not shielded, which might be a reasonable assumption. On this assumption the agreement between calculation and measurement is very good.

### 3.2 HERA

The absorbed energy fractions for various accelerator components of the HERA dipole magnet are shown in Fig. 8 as a function of the thickness of the lead shield. The geometry used in the calculation is shown in Fig. 2. The thickness of the lead shield was assumed to be the same on both radial sides of the vacuum chamber. No lead shield was mounted on the above and the bottom of the chamber. The vacuum chamber was assumed to be made of copper, as suggested in ref. 8, and had wall thickness of 4 mm.

Because of a good shielding effect of the copper vacuum chamber, it absorbs 93% of the synchrotron radiation energy. Since the lead shield is outside the chamber, the value is inde-

pendent of the lead thickness. The fraction of energy absorbed by the magnet yoke hardly changes as a function of the lead thickness. It is 5.2% at zero lead thickness and 4.3% above 2 mm. This is explained by the fact that most of the synchrotron radiation energy is absorbed in the vacuum chamber and that the absorbed energy fraction for the lead shield inside the yoke increases only slightly as a function of lead thickness, i.e. from 1.1% at 2 mm to 1.2% at 5 mm. This fact also indicates that even though the lead shields are added to the top and the bottom of the vacuum chamber, the absorbed energy fraction in the yoke would not be reduced much in the present case.

The fraction of energy leaving the magnet gap and one absorbed in the excitation coil decrease drastically as the lead thickness increases. At 5 mm lead thickness the fraction of energy is decreased by a factor of 50 less than that at 0 mm, and the latter by a factor of 30. Without lead shield the absorbed dose to the coil reaches  $2.6 \times 10^9$  rads on average for 25,000 h operation with a beam current of 56 mA, but is reduced to  $1 \times 10^8$  rads with 5 mm lead shield.

Absorbed dose to the coil insulation and to a component at the entrance of the magnet is plotted in Fig. 9 as a function of lead thickness. The former was calculated for two regions of interest (ROI), one of which was the region in front of the coil (ROI = 84) and the other behind (ROI = 106) (see Fig. 2). The values are normalized to an integrated current of  $1.4 \times 10^3$  A h, which was obtained assuming a running time of 25,000 hours with a beam current of 56 mA as stated above.

When the chamber is not shielded, the maximum absorbed dose to the coil insulator reaches  $1 \times 10^{10}$  rads for 25,000 hours operation. This is, however, reduced to  $3 \times 10^8$  rads, or by a factor of 30, when 5 mm thick lead shield is mounted on the radial side of the chamber. This amount of dose would not cause a serious radiation damage to the insulator. The ratio of absorbed doses to the insulator in front of and behind the coil is about 10, and it

is almost independent on the lead thickness.

The absorbed dose to a component at the opening of the magnet gap sums up to  $1.5 \times 10^{10}$  rad during the same period. The dose is strongly dependent on the lead thickness, and it could be reduced to  $2 \times 10^8$  rads with 5 mm thick lead. The absorbed dose to a component at the beam height and 1 m from the magnet gap is also plotted in Fig. 9.

Kötz<sup>11)</sup> has recently simulated the same problem for "HERA project with his Monte Carlo code in which only photoelectric and Compton scattering effects were taken into account. The code, however, included the polarization of the synchrotron radiation which the EGS code has not. Some of the present results are compared with his results in Table 4. They agree well with each other within a factor of 4, mostly 2. Larger discrepancies are thought to be caused by the differences in the geometry in both calculations and essential factors in both codes.

### 3.3 LEP

#### 3.3.1 Absorbed dose in various components

The LEP dipole magnet geometry used in the calculation is given in Fig. 3. The dimensions are not drawn in linear scale. The thickness of the ceramic insulation walls were fixed in the calculation. The lead thickness on the top and the bottom of the chamber was fixed at 3 mm whenever lead shield was added to the chamber. For zero lead thickness all the lead regions were filled with air.

The absorbed doses per integrated beam current of one Ah to a component at both radial regions (ROI = 9 and 174) of the vacuum chamber are plotted in Fig. 10 as a function of the thickness of the lead shield. The data in Table 1 show that the integrated current for ten years will be 276 Ah at 51.5 GeV operation assuming a 5000 hours run per year with a design beam current of 5.52 mA

per beam. Thus, the absorbed dose of  $10^8$  rads/Ah corresponds to the cumulated dose after ten years of  $(10^8 \text{ rads/Ah}) \times (276 \text{ Ah}) = 2.8 \times 10^{10}$  rads. The absorbed dose for any other periods can be obtained similarly.

Table 5 gives some of the absorbed dose values obtained from Fig. 10 for the regions in the air gap of the magnet. The region ROI = 9 is inside the beam orbit and the region ROI = 174 is outside. The dose reduction factor is the inverse of the ratio of the absorbed dose with lead shield to that without. The dose reduction factors for this region are less than those for the region 9 in spite of the thicker lead shield thickness. The reason for this feature can be easily understood if one considers the difference in the photon energy spectrum in both regions. See, for example, the photon energy spectra for the corresponding regions in the case of PETRA (ROI=D and A in Fig. 4). The spectrum in the region outside the beam orbit contains both higher and lower energy photons than that in the inside region. The photons in the inside region have been more multi-scattered from the point where the synchrotron radiation hits the vacuum chamber wall than those in the outside region. This is caused by the larger distance to the inside region from the impinging point and also by the geometry of the vacuum chamber.

The absorbed energy fractions to the vacuum chamber, excitation coil and ceramic insulator (only to the wall outside the beam orbit) and the energy fraction leaving the magnet gap are plotted as a function of the lead thickness in Figs. 11, 12 and 13 for operation energy of 51.5, 85 and 125 GeV, respectively. In any case the absorbed energy fraction to the vacuum chamber is independent of the lead thickness, as mentioned in section 3.1. The values are 0.58, 0.50 and 0.57 for 51.5, 85 and 125 GeV operations, respectively. The errors accompanied to them are far smaller than the differences among themselves. The absorbed energy fractions are not a simple linear function of energy, since the total energy impinging the vacuum chamber is normalized to unity in every case.



The error bars show the variation of the data in several runs of the program with different random number generation seeds, as stated in previous section.

Without shield the absorbed doses to the coil after a running time of ten years, or 50,000 hours, reach  $1.0 \times 10^9$  rads (52.5 GeV),  $1.9 \times 10^{10}$  rads (85 GeV) and  $5.8 \times 10^{10}$  rads (125 GeV). With these values and the graphs in Fig. 11 ~ 13 one can easily find the absorbed dose to the coil when a certain amount of the lead shield is added to the chamber.

At 51.5 GeV operation a 6 mm thick lead shield can reduce the absorbed energy fraction for the coil by a factor of 60 and the energy fraction leaving the magnet gap by 600. At 85 GeV the same thickness of lead can reduce the former by a factor of only 7 and the latter by 9. At 125 GeV operation it requires the lead thickness of 19 mm to reduce the absorbed dose fraction to the coil by a factor of 10, and 17 mm to reduce the energy fraction leaving the magnet gap by the same factor.

Since the magnet gap width is restricted, the thickness of the lead shield at the top and the bottom of the vacuum chamber is also limited. However, the thickness of 3 mm which was used in the present calculation might be enough if we take into account the results in the calculation for HERA (see section 3.2). The absorbed energy fraction for the ceramic insulator was given only for the wall outside the beam orbit where the absorbed dose is actually the highest among the other regions of the insulator.

### 3.3.2 Radial absorbed distribution

The radial absorbed dose at the beam height in the LEP tunnel was calculated using the same geometry<sup>4)</sup>, but of course not the same dimensions, as for PETRA. The results are shown in Figs. 14,

15 and 16 for the operation at 51.5, 85 and 125 GeV.

When no lead shield is provided to the vacuum chamber, the radial absorbed dose distribution decreases according to the inverse distance law in the case of 51.5 and 85 GeV operations. At 125 GeV operation it is well fitted by the inverse distance function (solid line) in the smaller distance regions ( $r < 60$  cm), but in larger distance regions it is better fitted by a function expressed by  $(1/r)^{0.8}$ .

Some of the reasons for above features are given as follows: Firstly, when the lead shield is added to the chamber, the dimensions of the "effective" radiation source becomes broader in the vertical direction because of its shielding effect and multiple scattering of the synchrotron radiation in the magnet yoke. Secondly, the shielding makes the outgoing spectrum harder, as shown in the previous section. This makes the radial absorbed dose distribution curve more flat.

Höfert<sup>12)</sup> has recently calculated the absorbed dose to a glass dosimeter at 1 m from the LEP machine. The results were  $5.4 \times 10^3$  rads/Ah at 51.5 GeV operation and  $9.3 \times 10^5$  rads/Ah at 85 GeV for the vacuum chamber shielded with 8 mm thick (outer side of the beam orbit) and 3 mm thick (inner side, bottom and top of the chamber) lead.<sup>\*</sup>) The corresponding values in the present calculation are, from Figs. 14 and 15,  $1.2 \times 10^4$  rads/Ah and  $1.0 \times 10^6$  rads/Ah at 51.5 GeV and 85 GeV operations, respectively. Both data agree well with each other.

---

<sup>\*</sup>) The original data are given for an operation of 5,000 hours with the beam current listed in Table 1 in the present paper.

#### 4. CONCLUSION

Based on the above results of the calculation the following remarks are given as conclusion.

##### 4.1 PETRA

- i) The calculated values by EGS3 of the absorbed dose to the glass dosimeter located in four regions inside and outside the dipole magnet gap agree within a factor of two with the corresponding values given from the measurement by Dinter and Tesch.
- ii) The calculated absorbed dose distribution in the radial direction at the beam height is expressed by  $(1/r)^{0.8}$ , where  $r$  is a distance from the surface of the vacuum chamber wall. It agrees with the experimental data well providing that there is 3% in length of the incomplete shielding sections along the storage ring.
- iii) The vacuum chamber absorbs 70% of the synchrotron radiation energy at 17 GeV operation and 54% at 21 GeV operation. Further, the energy deposition in the chamber is concentrated at the wall which the synchrotron radiation hits.

##### 4.2 HERA

- i) As much as 93% of the synchrotron radiation energy is absorbed by the 4 mm thick copper vacuum chamber. Because of this high absorbed energy fraction no lead shield would be required at the top and the bottom of the vacuum chamber.
- ii) When the chamber is not shielded, the cumulated absorbed dose to the coil insulation during 25,000 hours operation

reaches  $1 \times 10^9$  rads. This is reduced to  $3 \times 10^7$  rads with adding a 5 mm thick lead to the radial side of the chamber.

- iii) The absorbed dose to the coil during the same period reaches  $3 \times 10^9$  rads without shield and  $1 \times 10^8$  rads with 5 mm thick lead shield.
- iv) The absorbed dose to a component at the opening of the dipole magnet gap sums up to  $1.5 \times 10^{10}$  rads for 25,000 hours operation. Lead shield of 5 mm in thickness can reduce this value to  $2 \times 10^8$  rads.
- v) The present results agree well with the calculated values by Kötzt.

##### 4.3 LEP

- i) The absorbed energy fractions of the synchrotron radiation energy for the aluminum vacuum chamber are 0.58, 0.50 and 0.57 for 51.5, 85 and 125 GeV operation, respectively.
- ii) Without shielding the vacuum chamber the absorbed dose to the coil during ten years (a running time of 50,000 hours) reaches on average  $1.0 \times 10^9$  rads (51.5 GeV),  $1.9 \times 10^{10}$  rads (85 GeV) and  $5.8 \times 10^{10}$  rads (125 GeV).
- iii) At 51.5 GeV operation 6 mm lead shield can reduce the absorbed energy to the coil and the energy fraction leaving the magnet by a factor of 60 and 600, respectively. At 85 MeV, however, the same thickness can reduce them by a factor less than 10, giving the absorbed dose of  $7 \times 10^9$  rads to the coil during 10 years.
- iv) At 125 GeV even a 19 mm thick lead shield can reduce the

absorbed dose to the coil by a factor of only 10. Some other measures, such as filling the outside chamber region in the magnet gap by concrete, will have to be taken.

- v) Without shield the absorbed doses to a component at the opening of the dipole magnet during ten years arrives at the level of  $4.4 \times 10^9$  rads (52.5 GeV),  $2.7 \times 10^{10}$  rads (85 GeV) and  $4.9 \times 10^{10}$  rads (125 GeV). Those with lead shield can be obtained from the given figure in the text.
- vi) When no lead shield is provided to the vacuum chamber, the radial absorbed dose distribution decreases according to  $(1/r)$  or  $(1/r)^{0.8}$ . When the lead shield is added, the radial absorbed dose decreases less abruptly in the regions close to the vacuum chamber wall ( $r \approx 30 \text{ cm}$ ).

#### Acknowledgement

The author would like to express his sincere thanks to Dr. K. Tesch and Dr. H. Dinter for their help, useful advices and discussion. He is also grateful to Dr. E. Freytag for his encouragement.

#### References

1. J. Schwinger, On the classical radiation of accelerated electrons, *Phys. Rev.* 75, 1912 - 1925 (1949)
2. H. Dinter and K. Tesch, Some measurements of absorbed dose due to synchrotron radiation in the PETRA tunnel, DESY Internal Report D3/34, May 1981
3. R.L. Ford and W.R. Nelson, The EGS code system: Computer program for the Monte Carlo simulation of electromagnetic cascade showers (version 3), SLAC Report No. 210 (1978)
4. C. Yamaguchi, A manual for the EGS3 user code at DESY for Synchrotron Radiation Problem, DESY Internal Report, DESY D3/39 (1981)
5. K.R. Kase and W.R. Nelson, Concept of radiation dosimetry, SLAC Report No. 153 (1972)
6. C. Yamaguchi, Comparison of absorbed dose to RPL glass dosimeter calculated by EGS code and kerna, DESY Internal Report, DESY D3/40 (1981) (to be published in journal)
7. E. Storm and H.I. Israel, Photon cross sections from 1 KeV to 100 MeV for elements  $Z = 1$  to  $Z = 100$ , *Atom. Data and Nucl. Data Tables* 7, 565 (1970)
8. HERA, A proposal for a large electron-proton colliding beam facility at DESY, DESY HERA 81/10 (1981)
9. Design Study of a 22 to 130 GeV  $e^+e^-$  colliding machine (LEP), CERN/ISR-LEP/79-33 (1979)
10. A. Hutton, Parameter list for LEP version 11, LEP Note 289, CERN (1981)

11. U. Kötzt, Energy deposition and dose calculations for synchrotron radiation produced in the HERA bending magnet, DESY HERA 81/09 (1981)

12. M. Höfert, Some basic ideas on doses and dose distribution in the LEP tunnel, CERN RP Group Internal Report, HS-RP/TR/81-24 (1981)

Table 1 Some useful parameters concerned with the synchrotron radiation from PETRA, HERA and LEP

	PETRA	HERA	LEP		
			Stage I		Stage II
Energy (GeV)	19	30	51.5	85.0	125
Bending radius (m)	192	550	3104	3104	3104
Critical energy (keV)	79.2	109	97.6	439	1396
Circulating current per beam (mA)	10	56	5.52	9.25	6.16
Synchrotron radiation loss/turn (MeV/turn)	60.0	130	200	1490	6960
Synchrotron radiation loss/m (keV/m)	52.1	37.6	10.3	76.4	357
Integrated current in 10 years* (Ah)	560	2800	276	463	308

\*Annual operation of 5000 hours

Table 2 Comparison of measured and calculated absorbed doses for the RPL glass dosimeters which were located at four positions (A-D) in the PETRA dipole magnet air gap (see ref. 2). The values are expressed in rads per integrated current of 100 mA.h.

Energy		Measurement point/Region of interest (ROI)			
		A/114	B/96	C/24	D/6
17 GeV	Measurement	$8.4 \pm 0.3 \times 10^3$	$4.8 \pm 1.2 \times 10^7$	$1.5 \pm 0.4 \times 10^6$	$6.6 \pm 0.9 \times 10^3$
	EGS3	$1.6 \pm 1.3 \times 10^4$	$2.0 \pm 0.3 \times 10^7$	$2.9 \pm 0.8 \times 10^6$	$2.9 \pm 2.5 \times 10^3$
21 GeV	Measurement	-	-	-	-
	EGS3	$2.6 \pm 0.7 \times 10^5$	$4.9 \pm 0.4 \times 10^7$	$1.8 \pm 0.3 \times 10^7$	$1.8 \pm 1.6 \times 10^4$

Table 3 Deposited energy fraction calculated by EGS3 of the synchrotron radiation from PETRA in various accelerator components, and absorbed dose (rad/100mAh) at 1m from the surface of the vacuum chamber

Component	Energy	17 GeV	21 GeV
Vacuum Chamber		0.70	0.54
Magnet Yoke		0.22	0.34
3mm Pb shield (inside yoke)		0.071	0.12
" (outside " )		0.002	0.001
Coil (inside yoke)		0.002	0.006
" (outside yoke)		$\sim 1 \times 10^{-4}$	$\sim 2 \times 10^{-4}$
Escaping the magnet		$\sim 2 \times 10^{-5}$	$\sim 3 \times 10^{-4}$
Dose at 1m: with 3mm Pb		$6 \times 10^2$	$5 \times 10^3$
without Pb		$1 \times 10^5$	$5 \times 10^5$

Table 4 Energy fraction of synchrotron radiation loss deposited in various components of the HERA dipole magnet and doses to them. Doses are normalised to an integrated current of  $1.4 \times 10^3$  A h.

	Without lead		with 5 mm thick lead	
	EGS3	Kötzt	EGS3	Kötzt
Energy fraction				
Vacuum chamber (Cu)	0.932	0.92	0.932	0.92
Lead shield	-	-	0.025	0.055
Yoke	0.05	0.066	0.04	0.02
Coil (Al)	0.004	0.01	$1.4 \cdot 10^4$	$3 \cdot 10^{-4}$
Coil insulation	$1 \cdot 10^{-4}$	$4 \cdot 10^{-4}$	$1 \cdot 10^{-5}$	$1 \cdot 10^{-5}$
Leaving magnet gap	$1.4 \cdot 10^{-2}$	$6 \cdot 10^{-3}$	$3 \cdot 10^{-4}$	$2 \cdot 10^{-4}$
Doses (rads) to Coil insulation	$1.0 \cdot 10^{10}$	$3 \cdot 10^{10}$	$3.0 \cdot 10^8$	$8 \cdot 10^8$
Components at magnet opening	$1.6 \cdot 10^{10}$	$1 \cdot 10^{10}$	$3.0 \cdot 10^8$	$3 \cdot 10^8$

FIGURE CAPTIONS

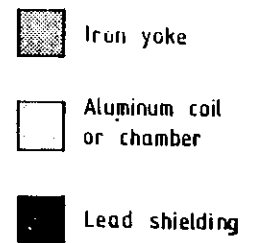
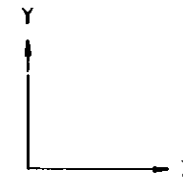
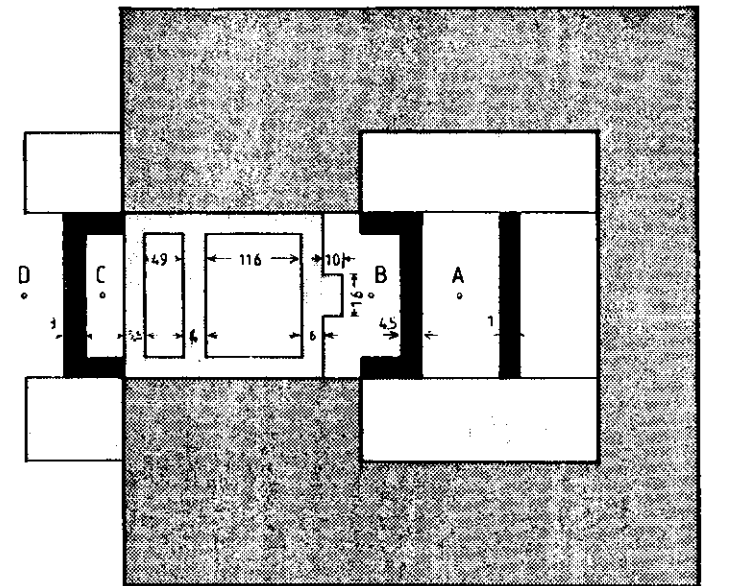
- Fig. 1 Geometry used in the calculation of the absorbed dose and deposited energy fraction for PETRA.
- Fig. 2 Geometry used in the calculation of the absorbed dose and deposited energy fraction for HERA.
- Fig. 3 Geometry used in the calculation of the absorbed dose and deposited energy fraction for LEP.
- Fig. 4 Photon spectra in various regions of interest (ROI) in the air gap of the PETRA dipole magnet at 17 GeV operation.
- Fig. 5 Deposited energy fraction in various parts of the PETRA vacuum chamber at 17 GeV operation.
- Fig. 6 Radial absorbed dose distribution in the PETRA tunnel (17 GeV).
- Fig. 7 Comparison of calculated and measured radial dose distribution in the PETRA tunnel. The solid line was drawn by eye.
- Fig. 8 Absorbed energy fractions in various magnet components of HERA at 30 GeV operation.
- Fig. 9 Absorbed dose to a component at the entrance of the HERA magnet gap, at 1 m from the magnet gap, and absorbed dose to the coil insulation. Operation energy is 30 GeV.
- Fig. 10 Absorbed dose to a component at both sides of the LEP vacuum chamber as a function of the lead shield thickness. The region ROI = 9 is inside the beam orbit and ROI = 174 is outside.
- Fig. 11 Absorbed energy fraction for the various components of the LEP dipole magnet as a function of the lead shield thickness. The operation energy is 51.5 GeV.
- Fig. 12 Absorbed energy fraction for the various components of the LEP dipole magnet as a function of the lead thickness. The operation energy is 85 GeV.

Table 5 Some of the absorbed dose values and the dose reduction factors for the regions in the air gap of the magnet

Energy (GeV)	ROI = 9 (Inside the beam orbit)				ROI = 117 (Outside the beam orbit)				
	400	30	7	150	25	5	125	85	
Absorbed dose (rad/Ah)									
Without Lead	$1.7 \times 10^7$	$6.0 \times 10^7$	$1.5 \times 10^8$	$5.0 \times 10^7$	$2.2 \times 10^8$	-	$5.5 \times 10^8$	$2.2 \times 10^8$	$2.2 \times 10^8$
With 8 mm Lead	$4.0 \times 10^4$	$2.2 \times 10^6$	$2.3 \times 10^7$	-	-	-	-	-	-
With 10 mm Lead	-	-	-	$3.2 \times 10^4$	$8 \times 10^6$	$1 \times 10^8$	-	-	-
Dose reduction factor	400	30	7	150	25	5	125	85	125

- Fig. 13 Absorbed energy fraction for the various components of the LEP dipole magnet as a function of the lead thickness. The operation energy is 125 GeV.
- Fig. 14 Radial absorbed dose distribution as a function of a distance from the surface of the vacuum chamber of LEP.
- Fig. 15 Radial absorbed dose distribution as a function of a distance from the surface of the vacuum chamber of LEP.
- Fig. 16 Radial absorbed dose distribution as a function of a distance from the surface of the vacuum chamber of LEP.

## PETRA

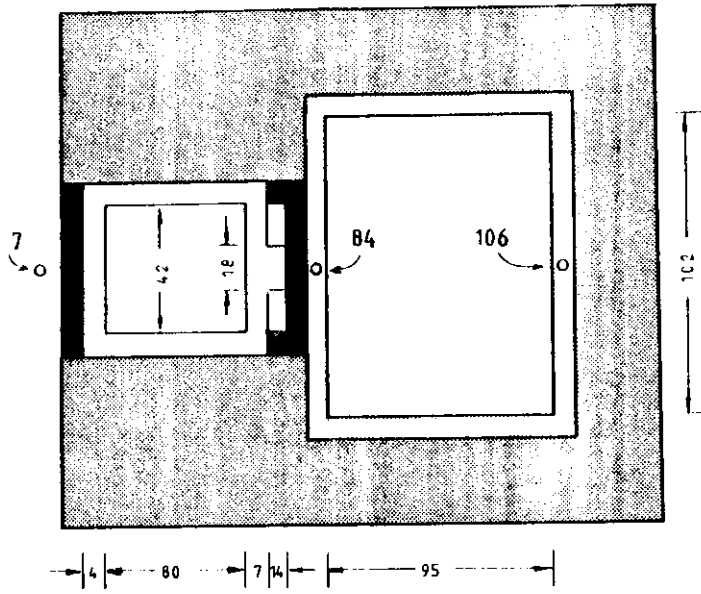






Scale in mm

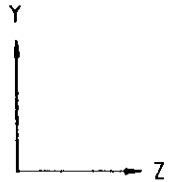
FIG 1

33119

### HERA



-  Iron yoke
-  Vacuum chamber or coil
-  Insulator
-  Lead shield

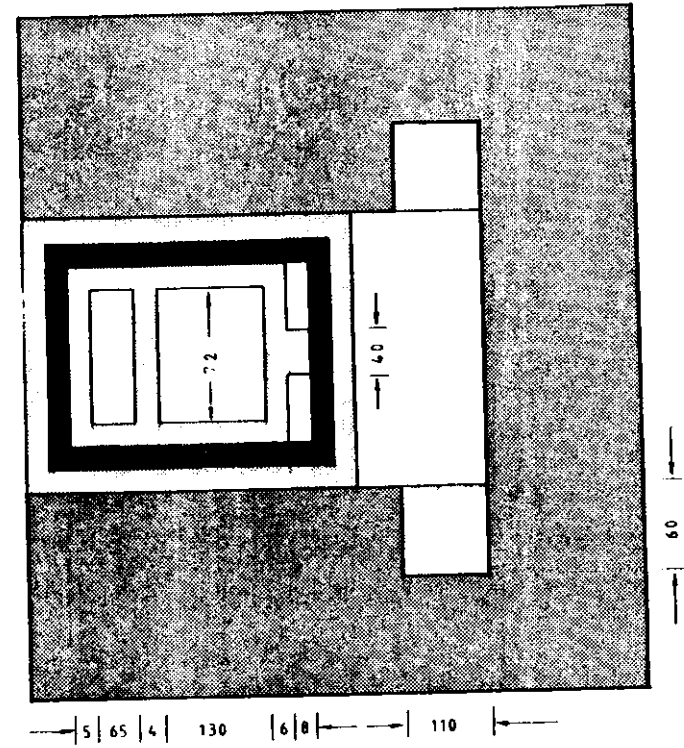






Units: mm

### FIG 2

33121

### LEP



-  Iron yoke
-  Ceramics heat insulation
-  Lead shield
-  Aluminum coil or chamber

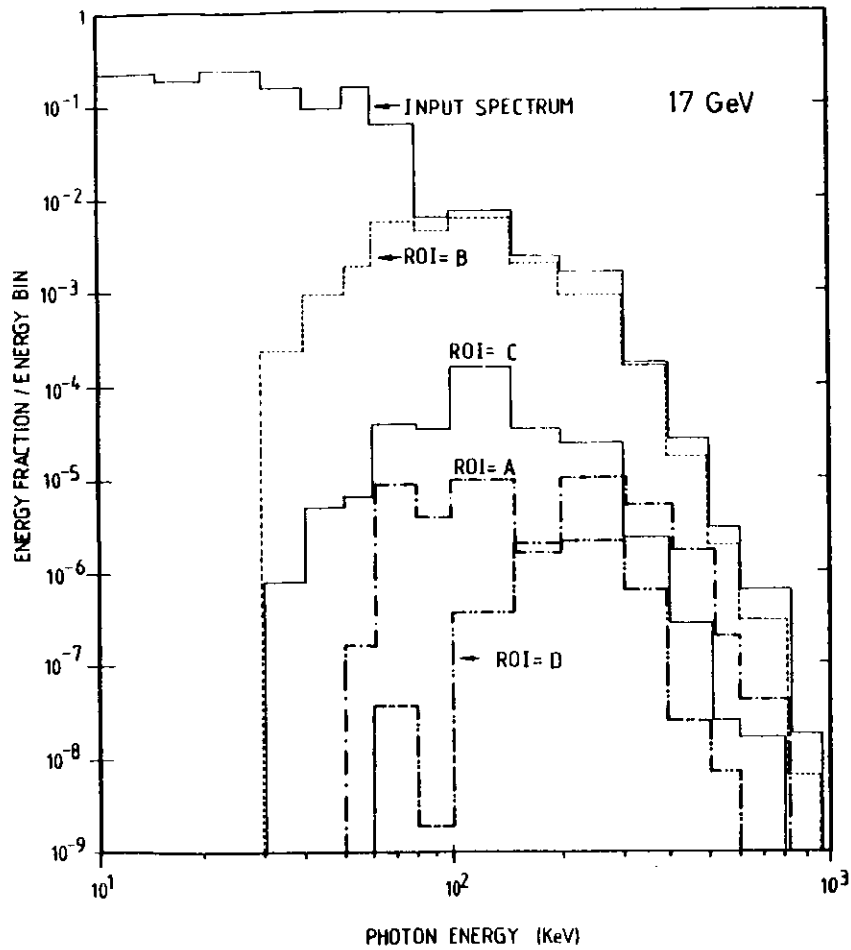


Units: mm

### FIG 3

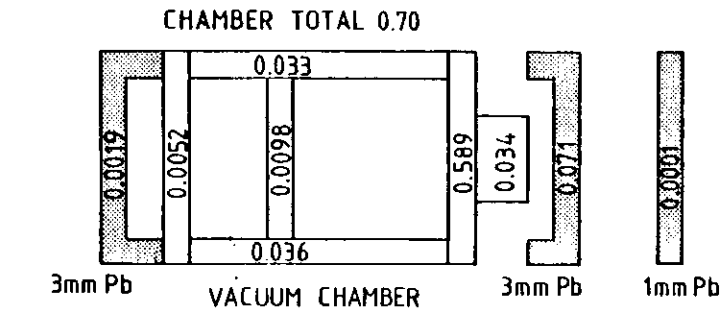
33120



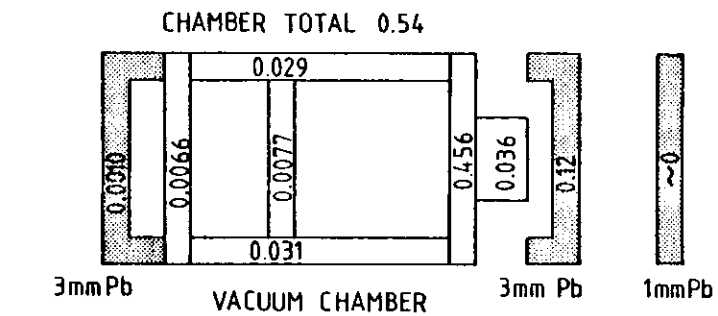


33123

FIG 4



a) DEPOSITED ENERGY FRACTION AT 17 GeV (PETRA)



b) DEPOSITED ENERGY FRACTION AT 21 GeV (PETRA)

FIG 5

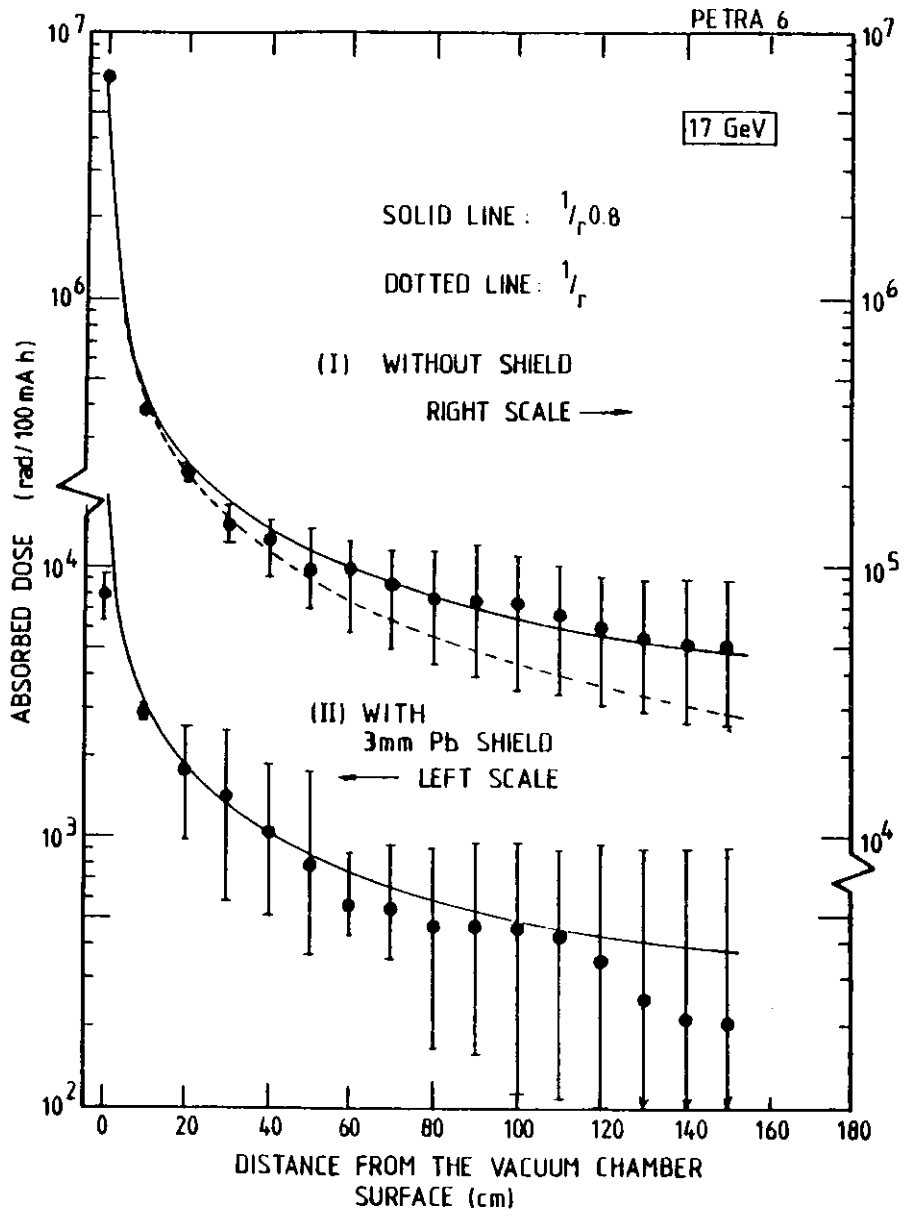


FIG 6

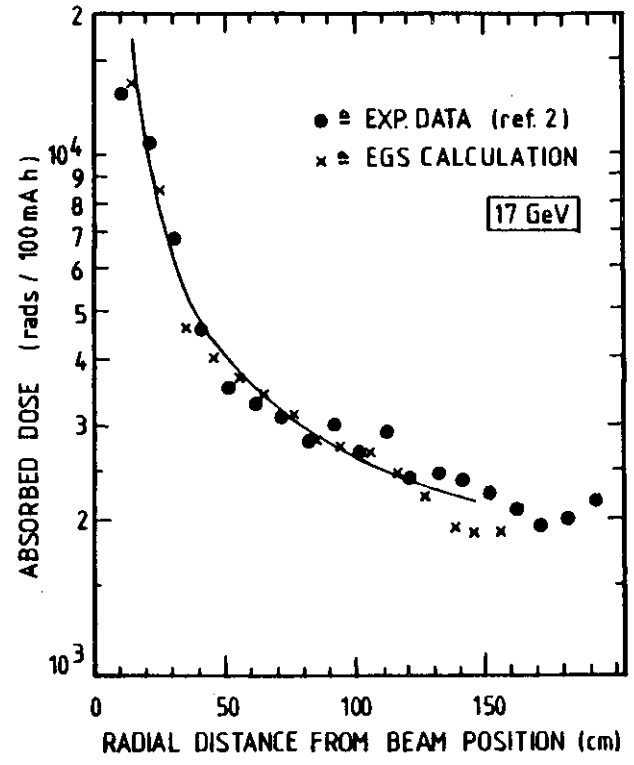


FIG 7

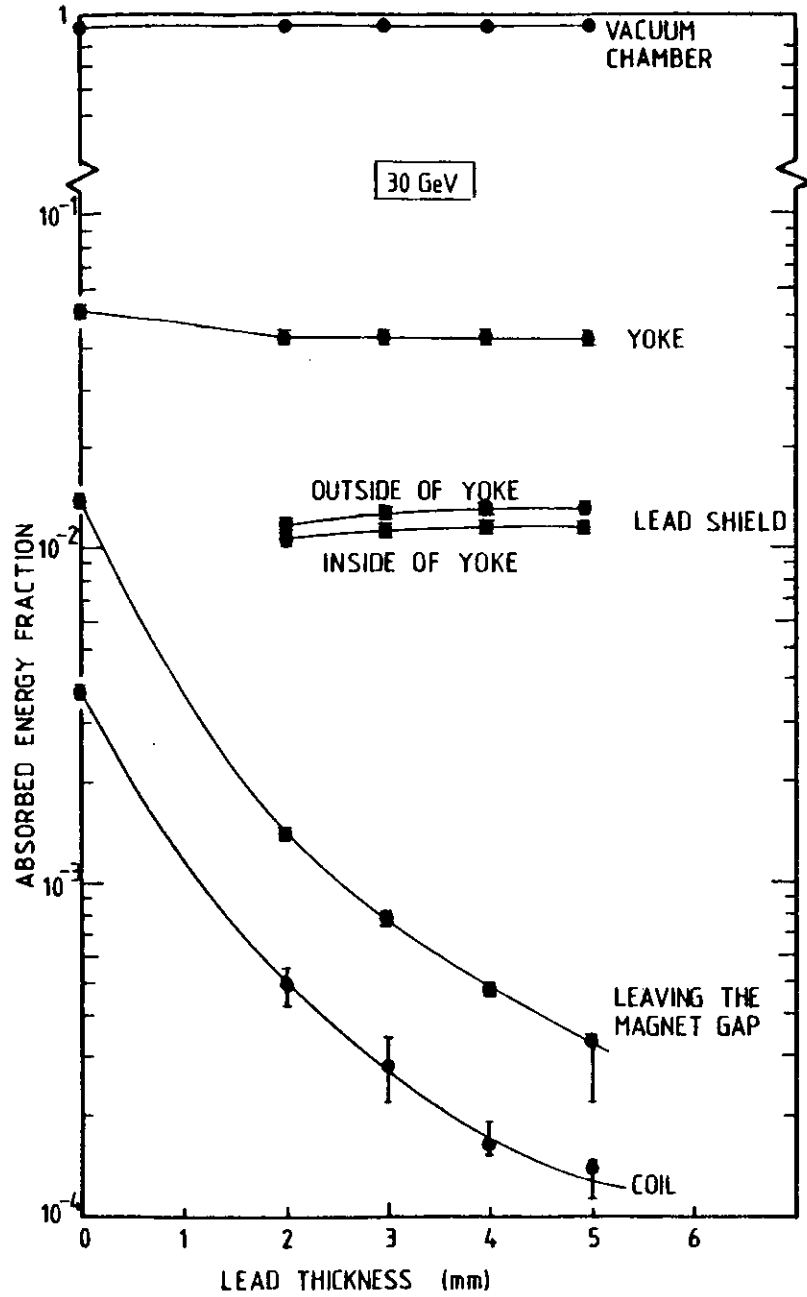


FIG 8

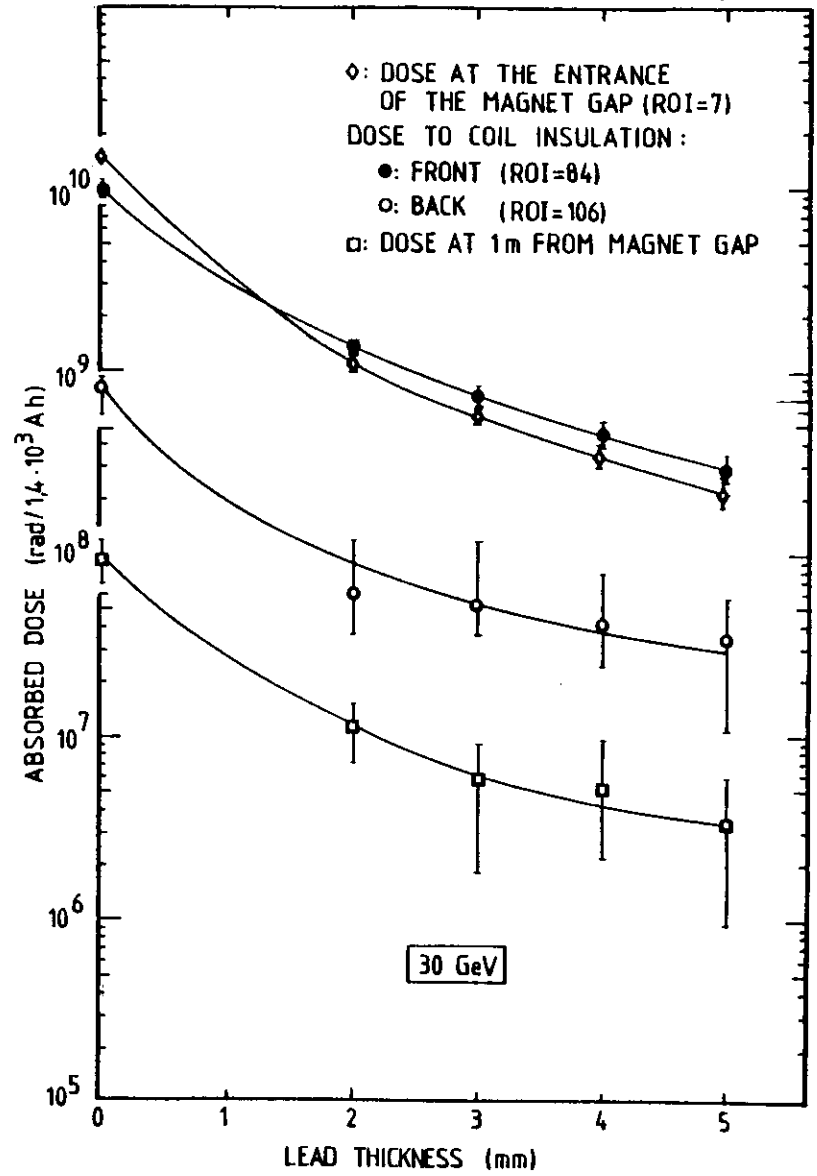


FIG 9

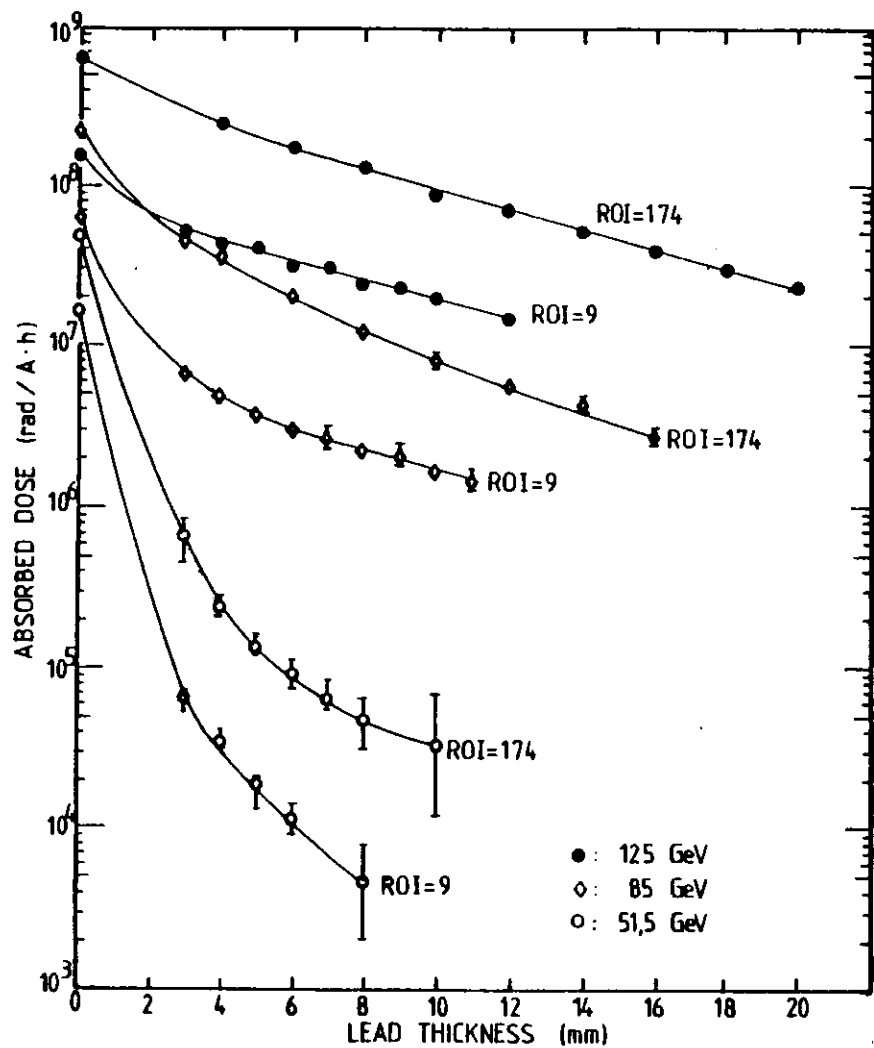


FIG 10

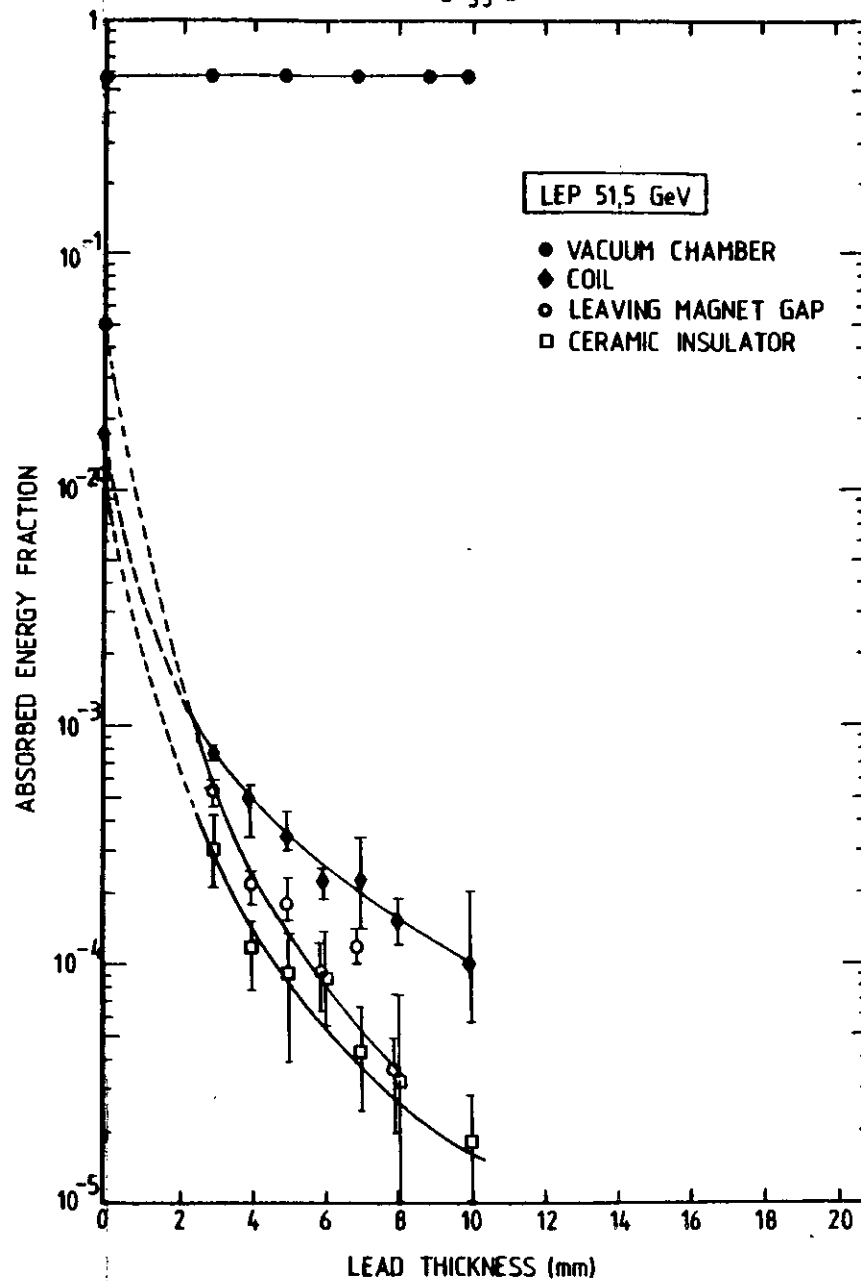


FIG 11

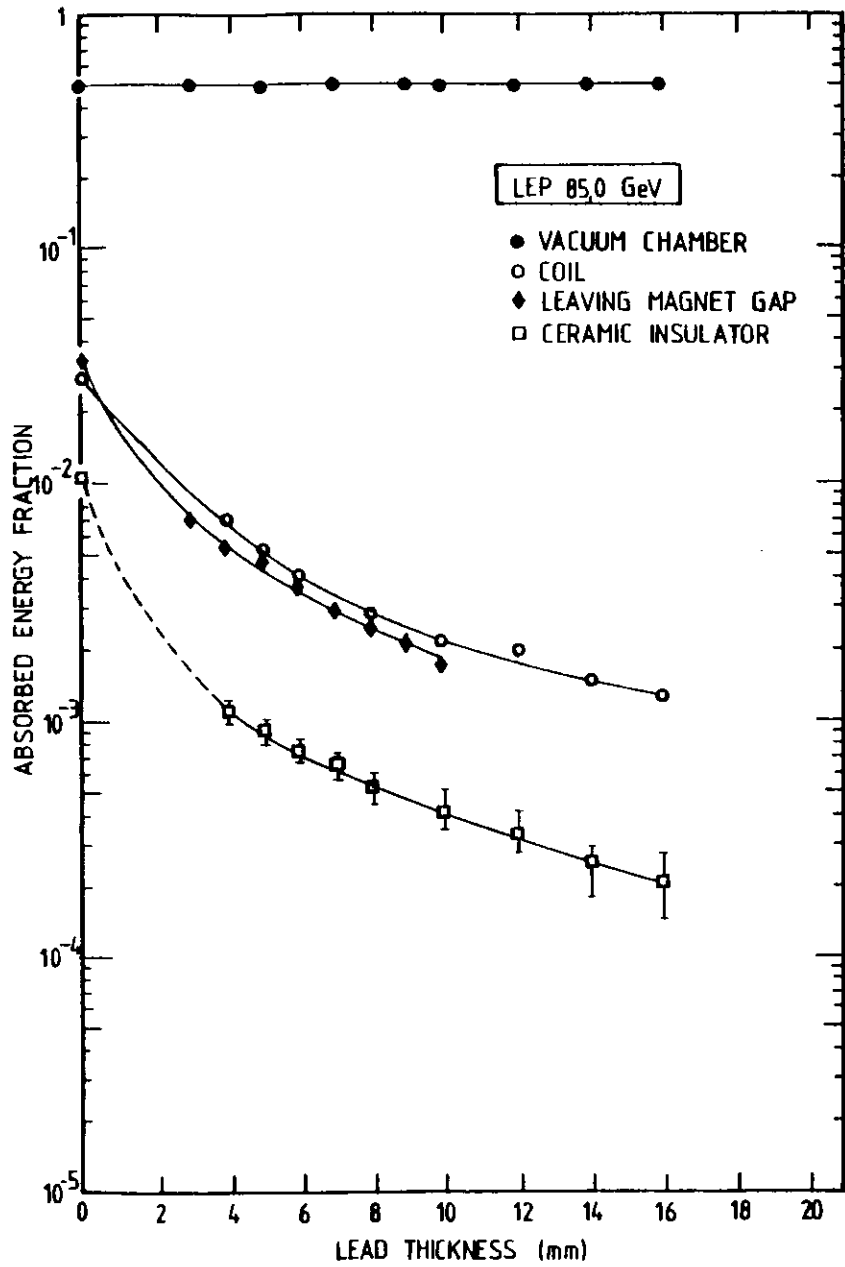


FIG 12

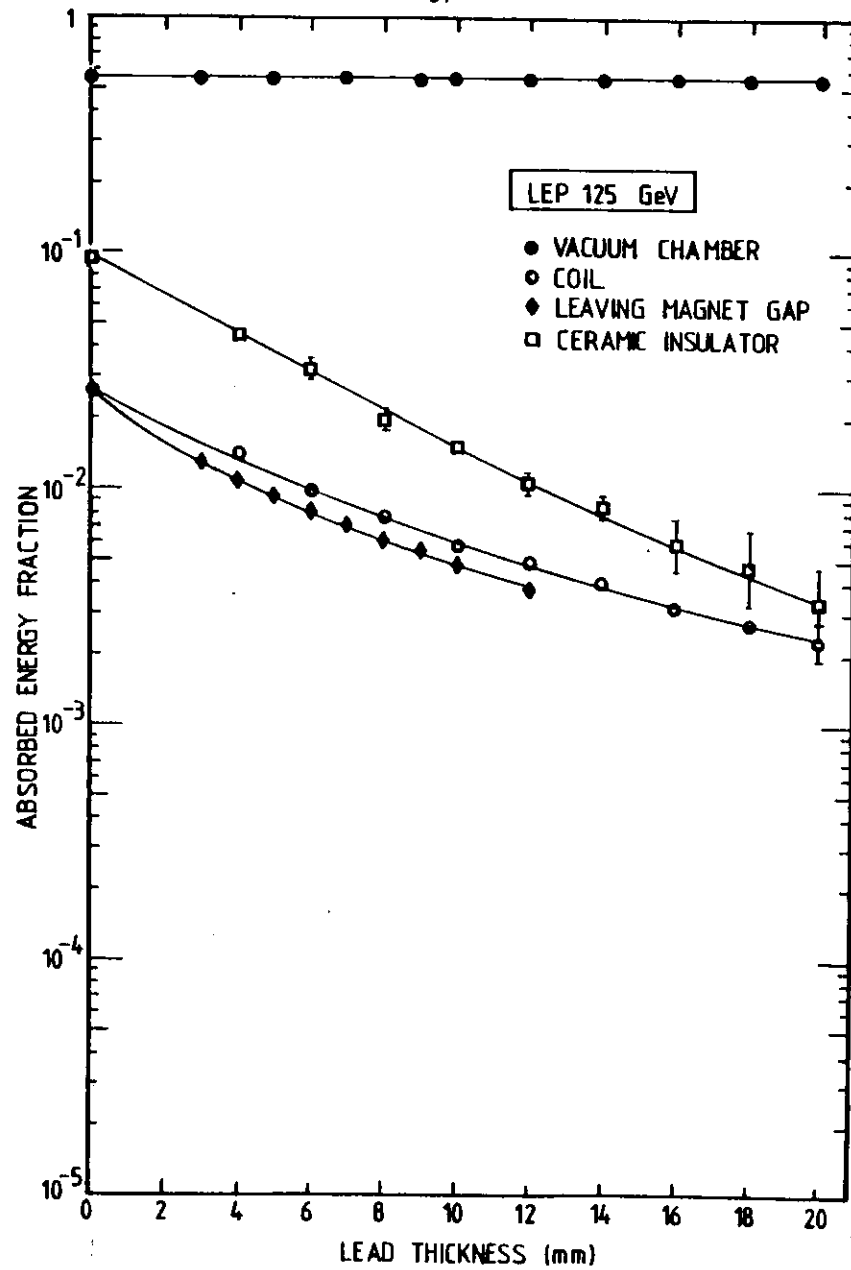


FIG 13

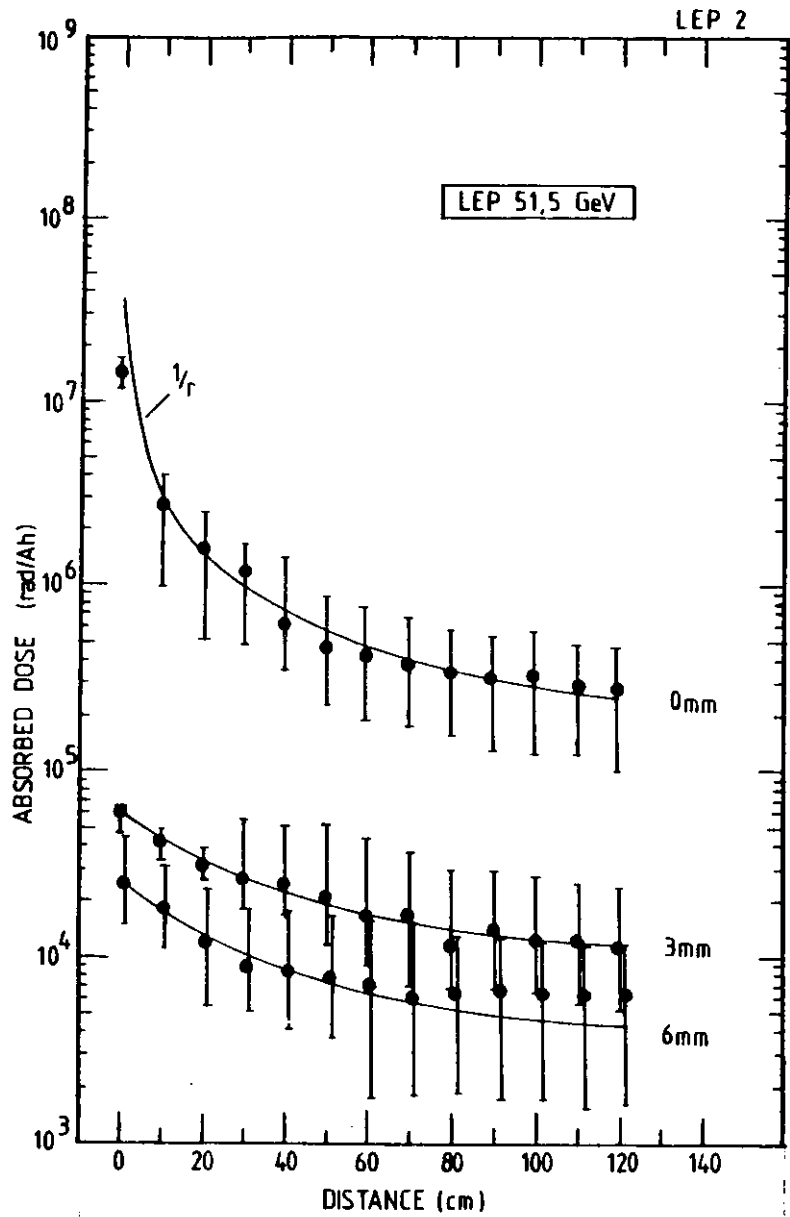


FIG 14

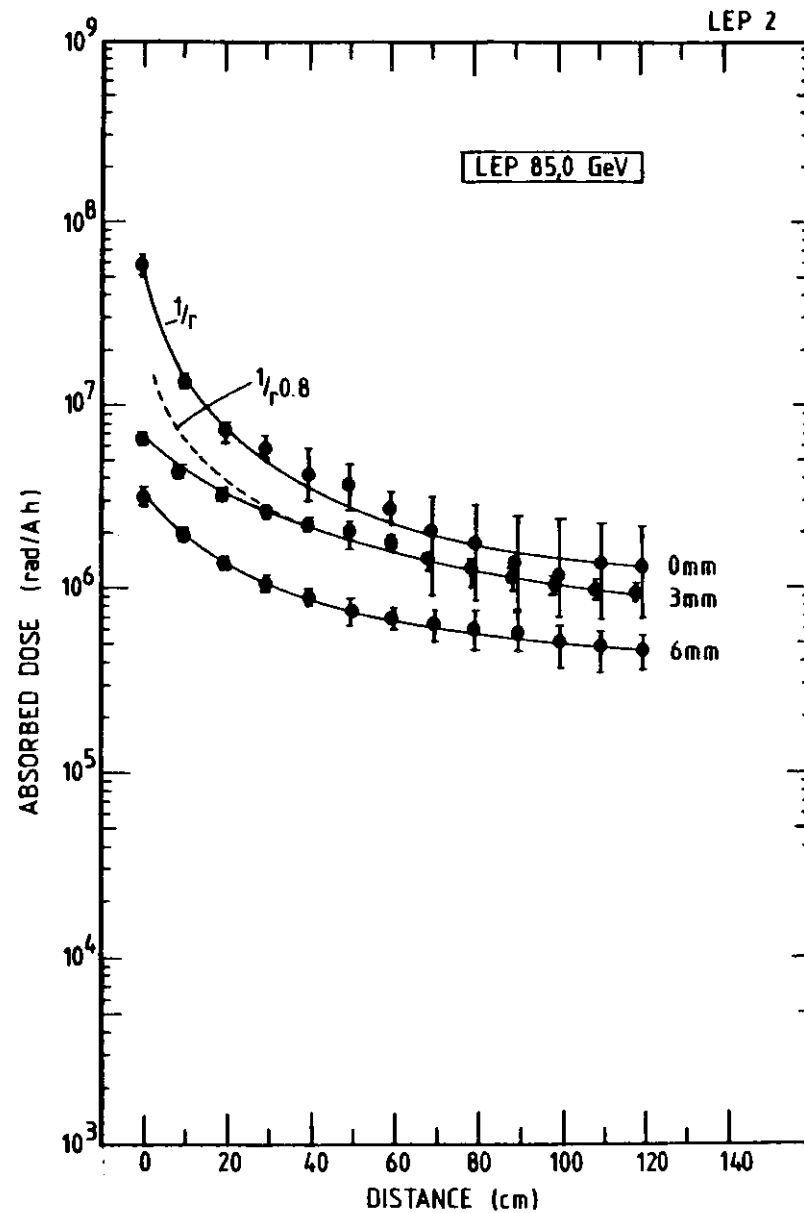


FIG 15

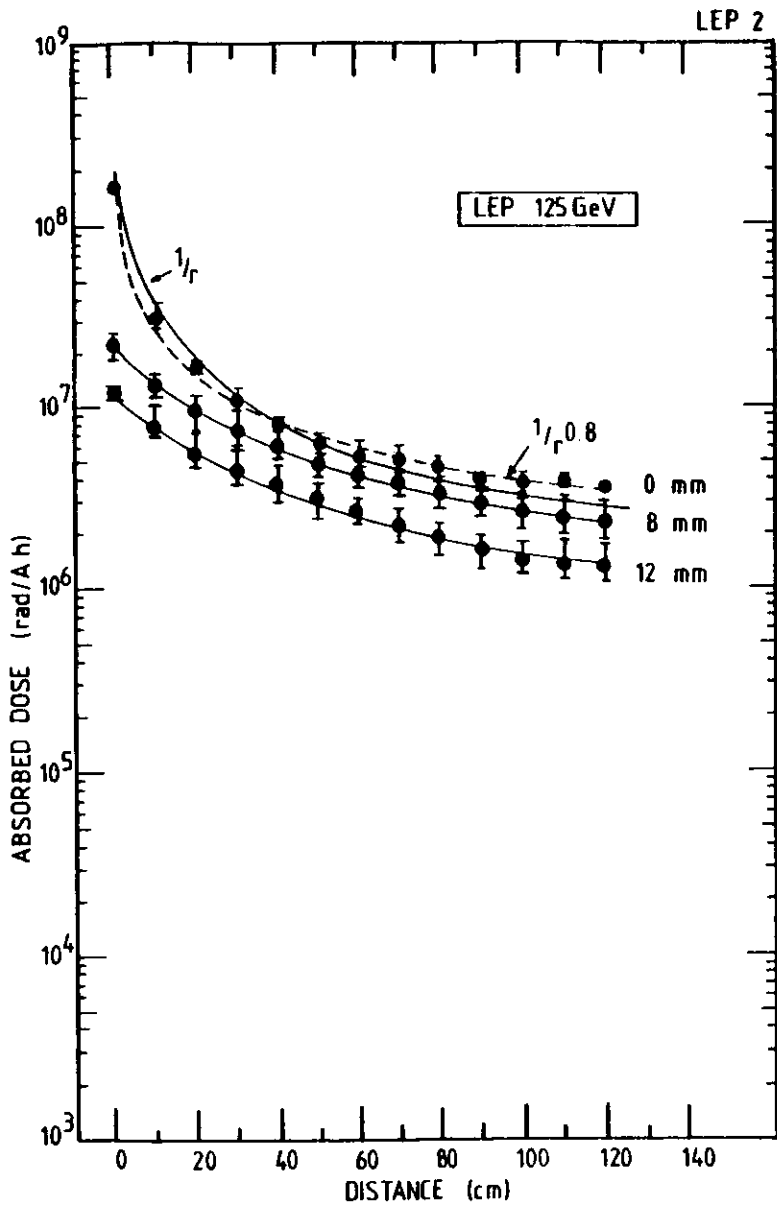


FIG 16

